Alternatives In The Generation Of Time Domain Models Of Fluid Lines Using Frequency Domain Techniques

Wayne J. Book
Georgia Institute of Technology
Atlanta, GA 30332-0405, U.S.A.

Cody Watson
Lockheed-Martin Co.
Fort Worth, TX U.S.A.

Abstract. By converting from frequency domain models to time domain models, nonlinear behavior and linear distributed behavior can both be effectively represented. Three methods are presented to convert fluid line models from the frequency domain to the time domain. Comparison shows that combination of components in the frequency domain has advantages in accuracy and efficiency in many practical cases. Methods of finding model poles and residues and ways to avoid numerical difficulties with poles at the origin are discussed.

Introduction.

Distributed components and systems are sometimes well described by linear partial differential equations and can thus be analyzed by frequency domain approaches. Frequency domain techniques allow the combination into a system model of linear components both distributed and lumped. One may prefer to convert the frequency domain model back to a finite order model for purposes of analysis, control or system design, or because additional components need to be included which are nonlinear and hence cannot be accurately modeled in the frequency domain.

Modeling pressure transients in fluid lines is an example of the general modeling task described above. This paper treats the modeling of fluid lines specifically but flexible structures [1] and other engineering systems are similar in their modeling needs. The fluid lines studied here might appear in a variety of engineering systems such as automobiles [3] and airplanes (fuel injection, brake lines, transmissions) and manufacturing equipment (hydraulic power lines).

This paper will present the techniques used to model a small number of components combined into a linear system. The overall process will be described but the focus of the paper will be on several issues that can form obstacles to the modeler. Comparisons will be made between three versions of this approach. Firstly, frequency domain component models can be immediately converted to time domain models, then combined with other time domain models. This is referred to as the Time Domain Combination (TDC) approach. The analytical conversion of the frequency domain model to the time domain produces the TDC-AC approach. Secondly, frequency domain models can be Numerically Converted to produce time domain approximations leading to the TDC-NC approach. Finally, the components can be combined in the frequency domain and numerically converted to the time domain (FDC-NC). Each approach has its own appeal. The modeling process was implemented in MATLAB © and Simulink © to obtain numerical and graphical support needed.

The paper will first describe briefly the components of the systems at hand. The fluid line is the only distributed component and will be treated in the most detail. Causality of the model becomes an important issue when components are combined. The conversion of the frequency domain component model will then be discussed. This technique has been explored in considerable detail in prior papers. Some new approaches have been applied to finding the residues, however. Then the frequency domain combination will be described. The numerical conversion (FDC-NC) will be discussed in detail. Finally, the results will be compared for a standard "water hammer" effect, the solution of which is analytically known for comparison. More detail is found in [8].

Fluid Line Component Models

Simple linear lumped parameter components, resistances, capacitances and inductances are important and result from ordinary differential or algebraic equations. The resistance, capacitance, and inductance, for example, are modeled as

$$\begin{bmatrix} P_a \\ Q_a \end{bmatrix} = \begin{bmatrix} 1 & R \\ 0 & 1 \end{bmatrix} \begin{bmatrix} P_b \\ Q_b \end{bmatrix} \qquad \begin{bmatrix} P_a \\ Q_a \end{bmatrix} = \begin{bmatrix} 1 & 0 \\ Cs & 1 \end{bmatrix} \begin{bmatrix} P_b \\ Q_b \end{bmatrix} \qquad \begin{bmatrix} P_a \\ Q_a \end{bmatrix} = \begin{bmatrix} 1 & Ls \\ 0 & 1 \end{bmatrix} \begin{bmatrix} P_b \\ Q_b \end{bmatrix} \tag{1}$$

where:

P_a, P_b = upstream and downstream pressure, respectively
Q_a, Q_b = upstream and downstream flow, respectively
R = resistance value; C = capacitance value; L = inductance value

A distributed fluid line is considerably more complex, and based on partial differential equations. This paper uses the dissipative or "exact" model[3] to describe fluid flow in a line. For this model, the fluid equations governing the flow in a differential boundary within a cylindrical fluid line are:

Momentum $$\rho_0 \frac{\partial u}{\partial t} + \frac{\partial p}{\partial x} = \mu_0 \left[\frac{\partial^2 u}{\partial r^2} + \frac{1}{r} \frac{\partial u}{\partial r} \right] \quad (2)$$

Continuity $$\frac{\partial \rho}{\partial t} + \rho_0 \left[\frac{\partial u}{\partial x} + \frac{\partial v}{\partial r} + \frac{v}{r} \right] = 0 \quad (3)$$

State $$\frac{d\rho}{\rho_0} = \frac{dp}{K_B} \quad (4)$$

where:

ρ_0, μ_0 = average density, absolute viscosity
u,v = axial, radial velocity
x,r = axial, radial coordinates
θ = temperature
K_B = bulk modulus

And we assume line length/line radius >> 1; small density change: $\Delta\rho / \rho_0 << 1$; radius of curvature of the line > radius of line and non-turbulent mean flow. There are simpler fluid property models that may be used, such as the inviscid or frictionless model and the linear friction model.

Much research has been done on the approximation of the dynamic response of liquid filled lines using the dissipative model[3,4,5,6,9]. This paper uses the same starting point as a basis for approximating the dynamic characteristics of a line, namely, the frequency domain representation[7] shown in Equations 5-9. Equation 9 is a general frequency domain transfer function relationship of the input and output flows, where *s* is the Laplace variable, $\Gamma(s)$ is the propagation operator, and $Z(s)$ is the characteristic impedance. Equation 5 is general because selecting either the inviscid, linear friction, or dissipative model produces the same representation with different expressions for $\Gamma(s)$ and $Z(s)$. The $\cosh(\Gamma(s))$ term is significant in that is represents the transmission of pressure or flow along the line. For instance $\cosh(\Gamma(s))$ produces a pure time delay in the inviscid model, while in the dissipative model it produces a time delay with frictional losses. The characteristic impedance provides a relationship of the flow at a point in the line to the corresponding pressure at that point[3].

$$\begin{bmatrix} P_a(s) \\ Q_a(s) \end{bmatrix} = \begin{bmatrix} \cosh(\Gamma(s)) & Z(s)\sinh(\Gamma(s)) \\ \frac{1}{Z(s)}\sinh(\Gamma(s)) & \cosh(\Gamma(s)) \end{bmatrix} \begin{bmatrix} P_b(s) \\ Q_b(s) \end{bmatrix} \quad (5)$$

Equations 6-9 represent the operators that form the dissipative model[3,7].

$$D_n = \nu_0 L / c_0 r^2 \quad (\bar{s}) = \frac{D_n \bar{s}}{\sqrt{1-B}} \quad (6)$$

$$\Gamma(\bar{s}) = \frac{D_n \bar{s}}{\sqrt{1-B}} \quad (7)$$

$$Z(\bar{s}) = \frac{Z_0}{\sqrt{1-B}} \quad (8)$$

$$B(\bar{s}) = \frac{2J_1\left(j\sqrt{\bar{s}}\right)}{j\sqrt{\bar{s}}J_0(j\sqrt{\bar{s}})} \quad (9)$$

where:

L = line length
ν_0 = mean kinematic viscosity
ρ_0 = mean fluid density
r_0 = radius of tube
D_n = dissipation number
J_0, J_1 = first and second order Bessel functions
K_B = Bulk modulus of the liquid

$Z_0 = \rho_0 c_0 / \pi r_0^2$ impedance constant

$c_0 = \sqrt{\frac{K_B}{\rho}}$ = fluid sonic speed

$\bar{s} = \frac{r^2}{\nu_0} s$ = normalized Laplace variable

Causality

If one thinks of the vector of variables on the right side of (5) as the input and the vector on the left as the output, the equation does not represent a causal physical system. Pressure and flow at the same location cannot be independently dictated at the same time. Algebraic manipulation can yield four alternative matirx equations in

causal form with seven distinct transfer functions. Equations 10-13 are the four possible causal conditions that can be formed from Equation 5[6].

$$\begin{bmatrix} P_a(s) \\ P_b(s) \end{bmatrix} = \begin{bmatrix} \frac{Z(s)\cosh(\Gamma(s))}{\sinh(\Gamma(s))} & -\frac{Z(s)}{\sinh(\Gamma(s))} \\ \frac{Z(s)}{\sinh(\Gamma(s))} & -\frac{Z(s)\cosh(\Gamma(s))}{\sinh(\Gamma(s))} \end{bmatrix} \begin{bmatrix} Q_a \\ Q_b \end{bmatrix} \tag{10}$$

$$\begin{bmatrix} P_a(s) \\ Q_b(s) \end{bmatrix} = \begin{bmatrix} \frac{Z(s)\sinh(\Gamma(s))}{\cosh(\Gamma(s))} & \frac{1}{\cosh(\Gamma(s))} \\ \frac{1}{\cosh(\Gamma(s))} & -\frac{\sinh(\Gamma(s))}{Z(s)\cosh(\Gamma(s))} \end{bmatrix} \begin{bmatrix} Q_a \\ P_b \end{bmatrix} \tag{11}$$

$$\begin{bmatrix} Q_a(s) \\ P_b(s) \end{bmatrix} = \begin{bmatrix} \frac{\sinh(\Gamma(s))}{Z(s)\cosh(\Gamma(s))} & \frac{1}{\cosh(\Gamma(s))} \\ \frac{1}{\cosh(\Gamma(s))} & -\frac{Z(s)\sinh(\Gamma(s))}{\cosh(\Gamma(s))} \end{bmatrix} \begin{bmatrix} P_a \\ Q_b \end{bmatrix} \tag{12}$$

$$\begin{bmatrix} Q_a(s) \\ Q_b(s) \end{bmatrix} = \begin{bmatrix} \frac{\cosh(\Gamma(s))}{Z(s)\sinh(\Gamma(s))} & -\frac{1}{Z(s)\sinh(\Gamma(s))} \\ \frac{1}{Z(s)\sinh(\Gamma(s))} & -\frac{\cosh(\Gamma(s))}{Z(s)\sinh(\Gamma(s))} \end{bmatrix} \begin{bmatrix} P_a \\ P_b \end{bmatrix} \tag{13}$$

Conversion to the Time Domain

The models derived above can be used in several different ways. For our current purposes we wish to convert the component model to a finite set of state space equations. This can be done by first expressing the transcendental transfer functions in partial fraction expansion as a truncated infinite series of first or second order transfer functions, each of which can directly be converted to a differential equation.

The first step in a partial fraction expansion is determination of the poles, followed by the determination of the residues which constitute the numerator of each first order partial fraction term. In particular when the poles are found numerically, the determination of the residues require some unusual approaches that will be now discussed.

Finding the Residues

In order to determine the residues r_i corresponding to the poles(p_i) of a transfer function, consider the partial fraction expansion of the a transfer function $F(s)$ represented as a ratio of polynomials in Equation 14:

$$F(s) = \frac{n(s)}{d(s)} = \frac{(s-z_1)(s-z_2)\ldots(s-z_{n-1})}{(s-p_1)(s-p_2)\ldots(z-p_n)} = \frac{r_1}{s-p_i} + \frac{r_2}{s-p_2} + \ldots + \frac{r_n}{s-p_n} \tag{14}$$

By multiplying Equation 14 by $s-p_i$ and finding the limit as s approaches p_i, the residue r_i can be represented as in Equation 15.

$$\lim_{s \to p_i} F(s)(s-p_i) = \lim_{s \to p_i} \left[\frac{r_1(s-p_i)}{s-p_1} + \frac{r_2(s-p_i)}{s-p_2} + \ldots + \frac{r_n(s-p_i)}{s-p_n} \right] = r_i \tag{15}$$

The term on the left side of Equation (15) is indeterminate at the poles and cannot be calculated directly since $F(s)$ and $s-p_i$ equal ∞ and 0, respectively, at $s=p_i$. When F(s) is given as a ratio of polynomials this is simply resolved by cancellation. This is not the case with the transcendental transfer functions here. As an alternative approach, the denominator can be represented by a Taylor series expansion around the poles.

$$d(s) = d(p_i) + d'(p_i)\frac{s-p_i}{1!} + d''(p_i)\frac{(s-p_i)^2}{2!} + \ldots \tag{16}$$

Simplifying this equation with the identity that $d(p_i)=0$, and dividing the equation by $s-p_i$ produces Equation 17.

$$\frac{d(s)}{s-p_i} = d'(p_i) + d''(p_i)\frac{s-p_i}{2!} + d'''(p_i)\frac{(s-p_i)^2}{3!} + \ldots \tag{17}$$

Now, by taking the limit of Equation 17 as s approaches p_i, the value of $d(p_i)/(s-p_i)$ is obtained as:

$$\lim_{s \to p_i} \frac{d(s)}{s-p_i} = \lim_{s \to p_i} d'(p_i) = d'(p_i) \tag{18}$$

Equation 19 is the derivative of the reciprocal of $F(s)$, simplified with the identity $d(p_i)=0$.

$$\left.\frac{d}{ds}\left[\frac{1}{F(s)}\right]\right|_{s=p_i} = \left.\frac{d}{ds}\left[\frac{d(s)}{n(s)}\right]\right|_{s=p_i} = \left.\frac{d'(s)n(s)-d(s)n'(s)}{(n(s))^2}\right|_{s=p_i} = \frac{d'(p_i)}{n(p_i)} \tag{19}$$

By substituting the reciprocal of Equation 18 into Equation 15, then applying the reciprocal of Equation 19, produces Equation 20.

$$\begin{aligned} r_i &= F(s)(s-p_i)\big|_{s=p_i} = \frac{n(s)}{d(s)}(s-p_i)\big|_{s=p_i} = \left[n(s)\frac{s-p_i}{d(s)}\right]_{s=p_i} \\ &= n(s)\left.\frac{1}{d'(s)}\right|_{s=p_i} = \left.\frac{n(s)}{d'(s)}\right|_{s=p_i} = \left.\frac{1}{\frac{d}{ds}\left[\frac{1}{F(s)}\right]}\right|_{s=p_i} \end{aligned} \tag{20}$$

This technique is useful when the transfer function can be calculated but is not in the form of a polynomial ratio. This method avoids the indeterminate condition as in Equation 15. For the hyperbolic transfer functions with Bessel function ratios, the values of the transfer function and its derivatives are easily obtained.

Time Domain Combination-Analytical Conversion (TDC-AC)

This will approach approximations at several steps as detailed in [6]. One approximation is the requirement for low viscosity. Evaluation of the Bessel functions and their ratio B is one example. B can be expressed as the ratio of two infinite products. The infinite product can then be substituted into the expressions for Z(s) and Γ(s) reduced to a product and ultimately an expression of the form

$$\frac{1}{\cosh(\Gamma)} = \sum_{i=1}^{k}\left[\frac{r_i}{(\bar{s}+p_i)}+\frac{r_i^*}{(\bar{s}+p_i^*)}\right] = \sum_{i=1}^{k}\left[\frac{a_i\bar{s}+b_i}{(\bar{s}^2+2\zeta_i\omega_i\bar{s}+\omega_i^2)}\right] \tag{21}$$

produces the complex poles of the transfer functions in (10)-(13). A similar process is required for 1/ sinh. Tabulated values [5] allow one to readily construct all of the transfer functions in those equations. From the simple transfer functions above a state space model can be constructed in one of several canonical forms.

Time Domain Combination-Numerical Conversion (TDC-NC)

The assumptions and approximations necessary to follow the TDC-AC may lead to questions of accuracy. Instead, the TDC-NC approach numerically searches for the values of the poles of the transfer functions in the component equations. Effectively a search is conducted for the zeros of cosh(Γ(s)) and sinh(Γ(s)), which are the denominators of the seven unique transfer functions. The MATLAB function fmins is used. Fmins employs a Nelder-Meads simplex algorithm.

It is necessary to produce suitable starting points for the numerical search. Consider the transfer function $1/\cosh(\Gamma(s))$. The relationship of cosine to its hyperbolic counterpart is: $\cos(x)=\cosh\left(x\sqrt{-1}\right)$. Also, it is known that the zeros of *cos(x)* occur at $x=n\pi/2$ where $n=1,3,\ldots$ and the value $\Gamma(s)=\frac{D_n s}{\sqrt{1-B}}\approx D_n s$ for low damping. Thus, the imaginary component of the pole can be approximated by:

$$\mathrm{Im}[p_{n,guess}]=\frac{2n-1}{2D_n}\pi i \tag{22}$$

The real part of the pole is approximated using a much more empirical formula:

$$\mathrm{Re}[p_{n,guess}]=\begin{cases}\dfrac{-1}{100D_n} & D_n \le 1\cdot 10^{-7} \\ \dfrac{1}{\sqrt{D_n}} & D_n > 1\cdot 10^{-7}\end{cases} \tag{23}$$

The purpose of Equations 22 & 23 is to provide guesses for the initial, low frequency poles. After the first pole is found, the subsequent guesses are extrapolated from the previous poles. The poles are assumed to be linearly spaced in the complex plane.

It is interesting to note that the Bessel functions become very large with increasing values of the imaginary portion of the argument argument. For instance $|J_1(100j)|=1.1\cdot 10^{42}$. For *1000j*, the value becomes too large to be represented by MatLab's IEEE *long* format ($>10^{308}$). Fortunately, MatLab has a convenient way to avoid this

problem. The function besselj has an optional argument that causes the answer to be divided by $e^{Im(arg)}$. This factor is canceled when the ratio of the Bessel functions is calculated. Thus, the ratio is calculated accurately without the necessity to represent ex remely large numbers.
The residues are again found using the method outlined in the section above. To use this method, the derivative of the transfer function must be calculated. For example, consider the transfer function $F(s)=\dfrac{\sinh(\Gamma(\bar{s}))}{Z(\bar{s})\cosh(\Gamma(\bar{s}))}$.
Equation 24 shows the manipulation of *F(s)*, with the identity that $\cosh(\Gamma\ (p_i)\neq 0$.

$$\left.\frac{n(\bar{s})}{d'(\bar{s})}\right|_{s=p_i}=\frac{\sinh(\Gamma(\bar{s}))}{\dfrac{d}{ds}\left[Z(\bar{s})\cosh(\Gamma(\bar{s}))\right]}=\frac{\sin(\Gamma(\bar{s}))}{Z(\bar{s})\Gamma'(\bar{s})\sinh(\Gamma(\bar{s}))}=\frac{1}{Z(\bar{s})\Gamma'(\bar{s})} \tag{24}$$

Equation 25 contains the derivative of $\Gamma(\bar{s})$, which is found to be:

$$\Gamma'(\bar{s})=\frac{d}{d\bar{s}}\frac{D_n\bar{s}}{\sqrt{1-B}}=D_n\frac{\sqrt{1-B}-\dfrac{\bar{s}}{2}(1-B)^{1/2}(-B')}{1-B}=\frac{1-B+\dfrac{B'\bar{s}}{2}}{(1-B)^{3/2}} \tag{25}$$

Equation 25 contains the derivative of the bessel function ratio *B*. The identities $J'_0(x)=-J_1(x)$ and $J'_0(x)=J_0(x)-J_1(x)/x$ and the substitution $x=j\sqrt{\bar{s}}\Rightarrow x'=\dfrac{1}{2\sqrt{\bar{s}}}$ are used to form the derivative of *B* in Equation 26.

$$B'=\frac{d}{d\bar{s}}\left[\frac{2J_1(x)}{xJ_0(x)}\right]=2\frac{J_1'(x)x'xJ_0(x)-J_1(x)(x'J_0(x)+xJ_0'(x)x')}{x^2J_0^2(x)}= \tag{26}$$

$$=B'=\frac{1}{2\bar{s}}\left[2-2B-\frac{\bar{s}}{2}B^2\right] \tag{27}$$

For transfer functions which contain poles located at the origin, the problem of determining the residue is complicated. Consider the transfer function $F(\bar{s})=\dfrac{Z(\bar{s})}{\sinh(\Gamma(\bar{s}))}$ which has a pole located at the origin. The residues are determined with Equation 27.

$$\left.\frac{1}{\dfrac{d}{d\bar{s}}\left[\dfrac{1}{F(\bar{s})}\right]}\right|_{s=p_i}=\left.\frac{Z(\bar{s})}{\Gamma'(\bar{s})\cosh(\Gamma(\bar{s}))}\right|_{s=p_i} \tag{28}$$

Evaluation of some of the parameters of Equation 27 are relatively simple for $\bar{s}=0$, as shown in Equation 28. In each case these values had to be obtained using L'Hopital's rule to evaluate the limit of the equation

$$B(0)=1 \qquad B'(0)=-\frac{1}{8} \qquad \Gamma(0)=0$$
$$\Gamma'(0^+)=\infty \qquad \Gamma'(0^-)=-j\infty$$

Clearly, Equation 27 is indeterminate since $Z=1/\sqrt{1-B}$ is infinite and $\Gamma(\bar{s})$ is infinite. Calculation of the limit of Equation 27 is algebraically involved. Fortunately, the symbolic limit of the equation may be obtained using the Symbolic Toolbox within MatLab. The limit in this case evaluates to Z_0/D_n. All residues for zero and nonzero poles for all seven distinct transfer functions have been analytically expressed in terms of the poles that will be numerically found. [8]

Frequency Domain Combination-Numerical Conversion (FDC-NC)

The strategy in the TDC approaches above is to enable standard techniques to convert to the time domain for a given component. A limited number of component modes are retained and the resulting system equation will have order equal to the sum of the order of all components. The accurate representation of N_s modes for the system will require more than N_s in total. This is essentially because the component modes are not system modes but effectively basis functions that allow the spatial variation of the system variables to be represented. The strategy with the current FDC approach is to combine components in the frequency domain where possible, retaining the infinite order transfer function. The transfer matrix representation of components in (1), and (5) make the serial combination a simple matter of multiplying these matrices together. The resulting equation form

is not causal. If the equations are converted to causal form an explicit relation between inputs and outputs is obtained. Alternatively, the noncausal form can be the basis for conversion to the time domain as shown in [1].

This paper has modified the previous work by incorporating new methods for solving for the residues. In the case of [1] it was necessary to use curve fitting techniques to find an appropriate residue, the numerator of the partial fraction expansions. Here the technique detailed above is much cleaner and more efficient. It does require analytical manipulation of the transfer functions using symbolic processing and that must be done for a given combination of components. Once completed however, the residues are explicitly known in terms of the values of the corresponding poles.

Numerical Example: Serial Combination of Fluid Lines

A simple but revealing example is to create a line model for two lines connected end to end, with an opening somewhere along the line as in Figure 1. The radii of the lines are equal and no restriction is made on the length of the lines. This selection allows comparison to known solutions in special cases. Combining the components and the conservation of flow and equality of pressure where the lines join produces a noncausal version of the model.

Equation 29 is not a realistic causality condition since both P_3 and Q_3 are specified. There are a number of ways this could be rearranged to produce a causal condition, for instance exchanging P_1 and P_3. In order to do this, consider the simple algebraic manipulation of the partitioned linear equation in Equation 30.

Figure 1. Two Fluid Line Element Combination

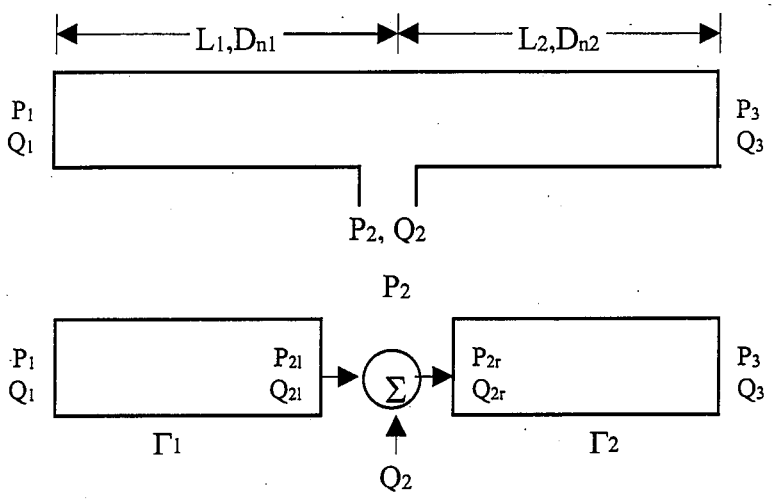

$$\begin{bmatrix} P_1(s) \\ Q_1(s) \\ P_2(s) \end{bmatrix} \begin{bmatrix} \cosh(\Gamma_1+\Gamma_2) & -Z\sinh(\Gamma_1) & Z\sinh(\Gamma_1+\Gamma_2) \\ \frac{1}{Z}\sinh(\Gamma_1+\Gamma_2) & -\cosh(\Gamma_1) & \cosh(\Gamma_1+\Gamma_2) \\ \cosh(\Gamma_2) & 0 & \cosh(\Gamma_2) \end{bmatrix} \begin{bmatrix} P_3(s) \\ Q_2(s) \\ Q_3(s) \end{bmatrix} \tag{29}$$

$$\begin{bmatrix} x_1 \\ x_2 \end{bmatrix} = \begin{bmatrix} A_{11} & A_{12} \\ A_{21} & A_{22} \end{bmatrix} \begin{bmatrix} y_1 \\ y_2 \end{bmatrix} \Rightarrow$$
$$\begin{bmatrix} y_1 \\ x_2 \end{bmatrix} = \begin{bmatrix} A_{11}^{-1} & -A_{11}^{-1}A_{12} \\ A_{21}A_{11}^{-1} & A_{22}-A_{21}A_{11}^{-1}A_{12} \end{bmatrix} \tag{30}$$

Applying the same manipulation from Equation 56 to Equation 55 produces the causal transfer function matrix in Equation 31.

$$\begin{bmatrix} P_3(s) \\ Q_1(s) \\ P_2(s) \end{bmatrix} = \begin{bmatrix} \frac{1}{\cosh(\Gamma_1+\Gamma_2)} & \frac{Z\sinh(\Gamma_1)}{\cosh(\Gamma_1+\Gamma_2)} & -Z\tanh(\Gamma_1+\Gamma_2) \\ \frac{\tanh(\Gamma_1+\Gamma_2)}{Z} & \frac{-\cosh(\Gamma_2)}{\cosh(\Gamma_1+\Gamma_2)} & \frac{1}{\cosh(\Gamma_1+\Gamma_2)} \\ \frac{\cosh(\Gamma_2)}{\cosh(\Gamma_1+\Gamma_2)} & \frac{Z\sinh(\Gamma_1)\cosh(\Gamma_2)}{\cosh(\Gamma_1+\Gamma_2)} & \frac{-Z\sinh(\Gamma_1)}{\cosh(\Gamma_1+\Gamma_2)} \end{bmatrix} \begin{bmatrix} P_1(s) \\ Q_2(s) \\ Q_3(s) \end{bmatrix} \tag{31}$$

Comparing (29) and (31) exposes one of the advantages of the causal form. From (31) the poles of the serial combination are clearly the values of s the are the roots of $\cosh(\Gamma_1 + \Gamma_2)$. This is clear regardless of the specification of inputs or boundary conditions on the variables chosen as the input.

In each of the transfer functions of Equation 31, the combination $\Gamma_1+\Gamma_2$ appears. By setting the intermediate flow to zero, the system is reduced to the basic system of one line with two ends and extra information about the pressure within the flow element. Further, if P_2 is ignored, Equation 31 takes on the exact form of a single line, verifying the equations.

Branched System

A further generalization involves branches in the fluid line as shown in Figure 2.

Figure 2. Three Line Branch System

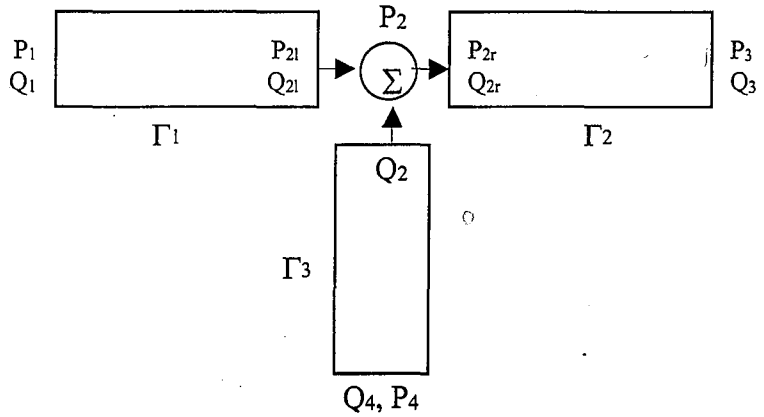

An example of a causal form is as follows:

$$\begin{bmatrix} Q_4(s) \\ P_3(s) \\ P_1(s) \end{bmatrix} = \frac{1}{K} \begin{bmatrix} -\sinh(\Gamma_2) & \cosh(\Gamma_1+\Gamma_2)\cosh(\Gamma_3)/Z + \cosh(\Gamma_1)\cosh(\Gamma_2)\cosh(\Gamma_3)/Z & -\frac{\cosh(\Gamma_1)}{Z} \\ \sinh(\Gamma_3) & \frac{\cosh(\Gamma_1)}{Z} & -\sinh(\Gamma_1+\Gamma_2)\sinh(\Gamma_3)/Z - \cosh(\Gamma_1)\cosh(\Gamma_2)\cosh(\Gamma_3)/Z \\ Z\sinh(\Gamma_1+\Gamma_2)\sinh(\Gamma_3)+ Z\sinh(\Gamma_1)\sinh(\Gamma_2)\cosh(\Gamma_3) & \sinh(\Gamma_2) & \sinh(\Gamma_3) \end{bmatrix} \begin{bmatrix} Q_1(s) \\ P_4(s) \\ P_3(s) \end{bmatrix} \quad (32)$$

where: $K = \cosh(\Gamma_1+\Gamma_2)\sinh(\Gamma_3)+\cosh(\Gamma_1)\sinh(\Gamma_2)\cosh(\Gamma_3)$.

Clearly, the roots of K are the poles of this system for any simple boundary conditions on the input variables. An analytical solution for these roots is not available but numerical searches for the roots is relatively straight forward. The techniques for finding the residues is again possible and is applied to the case of poles at the origin differently than the general case for poles elsewhere.

Choice of Time Domain Form

Two canonical forms are readily produced from a transfer function representation of second order dynamics: controllable form and observable form. In controllable form numerical problems can result due to poles at the origin. The steady state value of flow, for example, will depend on the difference between the integral of pressure at each of two inputs. Control canonical form integrates each pressure first then combines the result with a difference. As time gets large the two integrals must both become large and have a difference of zero to represent zero steady state flow. Observer canonical form combines the pressures prior to integration then integrates. Hence the numerical problems associated with a small difference of large numbers never arises.

Numerical Results and Comparison

The serial combination of lines has been simulated to give representative results to refer to when discussing the advantages of the three techniques described above. Properties were approximately those that would be found in automotive components such as fuel lines. The parameters used were are in the Table below.

Table 1: Parameters for Serial Line Combination

L_1	L_2	r_0	c_0	ν_0	ρ_0
15 cm	22.5 cm	6.35 mm	2848 m/s	3.52×10^{-7} cm	680 kg/m^3

The system will be subjected to a step pressure response at the open end of a line blocked at the other end. The result of applying a sudden pressure change at the end of a line is a pressure wave. This wave travels down the length of the line, and is reflected at the opposite end of the line, which is blocked. The nature of this wave is "square". With no friction, the wave would continue to reflect from end to end with this square shape. The dissipation used in our model causes the oscillations to decay with time. This decay slowly erodes the wave shape until no oscillations remain. At steady state, the pressure at the blocked end will be equal to the pressure at the open end, and the flow at the open end will be zero. This experiment is similar to the classic "waterhammer" example in which there is an initial steady non-zero flow which is abruptly stopped, for example with a valve. The simple nature of the exact response allows one to readily compare the simulations to reality.

Figures 3 and 4 show the response of Q_1 with Q_2 set to zero and a unit step applied to P_1. Figure 3 shows the initial response. All of the traces exhibit the same general response, with the ripple in the theoretically flat portions of the time response having higher amplitudes for Methods 1 (TDC-AC_) and 2 (TDC-NC) than for Method 3 (FDC-NC). The vertical dotted lines represent the wave travel time calculated simply from $T=2L/c_0$.

Figure 13 shows the response after 20 oscillations in the line. Both time domain combinations, Methods 1 and 2 exhibit the decay of the ``square" nature of the single element response. Additionally, the frequency of the reflection of the square wave is different from the predicted value in each of the two element models. The phase of the square wave response is deceptive from Figure 13, because after approximately 14 oscillations, Method 1 and Method 2 were 180^0 out of phase, with Method 2 more closely corresponding to the Method 3 model.

Conclusions

This paper has presented ways in which to model fluid line elements. The method of combination of individual models in the frequency domain before transformation into the time domain seems to provide improved performance of the model because of the ability to accurately represent modes of combined systems, instead of relying on the component modes of subsystems. For this reason, fewer modes are necessary to represent the behavior of the combined system. In the case considering branched lines with radically different lengths (not shown in this paper), the frequency domain combination model poorly represented short line dynamics.

Figure 3. Two Line Blocked Comparison, Initial Response

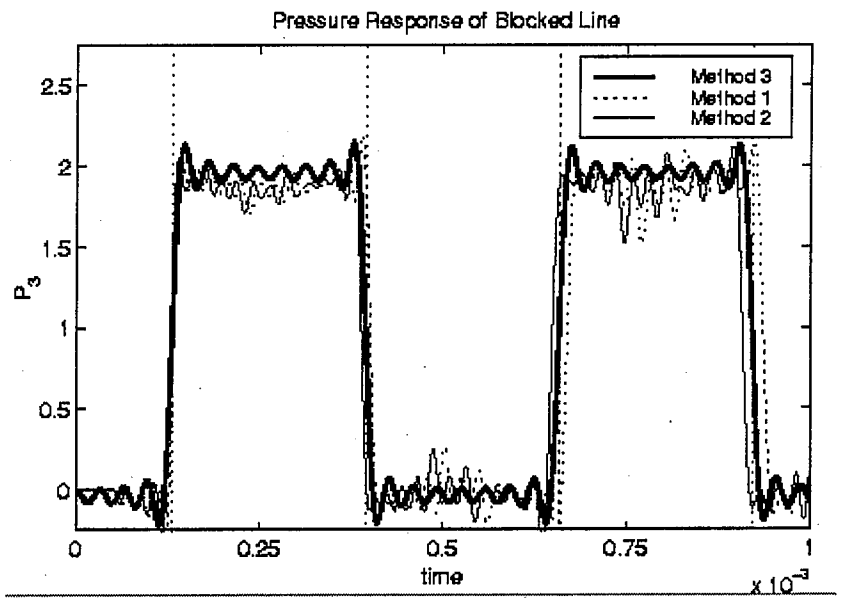

Figure 4. Two Line Blocked Comparison, Response After Twenty Cycles

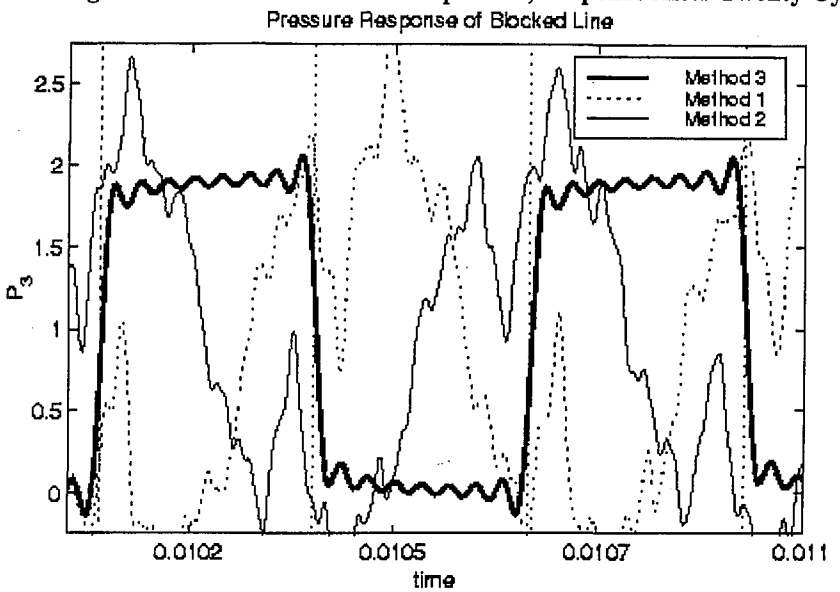

This paper has demonstrated that the combination of relatively few components in the time domain reduces the accuracy of the system response. Error is accumulated since the system is constructed of many subcomponents which are individually approximated, providing many sources for error. These errors can consist of numerical dispersion in the system, or artificially high amplitude, high frequency components. By increasing the number of modes in the subsystems, the errors can be reduced, but this requires the model to become increasingly large. Frequency domain combination attacks these problems at the source, component modes. For every frequency domain combination, one more set of component modes is eliminated. The case of widely differing line lengths presented a case where the construction of such a frequency domain model has practical difficulties. Thus, to construct a system, a hybrid approach must be used to form a complete system. This method would use frequency domain combination where practical, including many modes to improve the interaction with other subsystems. Additional details are found in [8].

Acknowledgements

Partial funding for this research was provided by a grant from Ford Motor Company.

References

1. Book, W. J. and Majette, M. Controller design for flexible, distributed parameter mechanical arms via combined state space and frequency domain techniques. *Journal of Dynamic Systems, Measurement and Control*, Vol 105, pp 245-254, December 1983.
2. Goodson, R. E. and Leonard, R.G. A survey of modeling techniques for fluid line transients. *Journal of Basic Engineering,* Transaction of ASME, 94, June 1972. Series D.
3. Glidwell, J. M., Yang, W.C. and Chuo, G. K. An on-board diagnostic strategy for multi-port electronic fuel injection systems using fuel transient analysis. ASME, Advanced Automotive Technologies, Vol 52, pp 257-265, 1993.
4. Heally, A. J. and Hullender, D. A. State variable representation of modeal approximations for fluid transmission line systems. *Journal of Dynamic Systems, Measurement and Control*, ASME, November 1981. Special Symposium on Volume of Fluid Transmission Line Dynamics.
5. Hsue, C. Y-Y and Hullender, D. A. Modal approximations for the fluid dynamics of hydraulic and pneumatic transmission liens. *Fluid Transmission Line Dynamics*, II, November 1983. ASME Special Publication, New York.
6. Hullender, D. A. and Heally, A. J. Rational polynomial approximations for fluid transmission line models. *Fluid Transmission Line Dynamics*, November 1981. Special Publication of the ASME Annual Winter Meeting, Washington, D.C.
7. Iberall, A. S.. Attenuation of oscillatory pressures in instrument lines. *Journal of Research*, 45 (R.P. 2115), July 1950. National Bureau of Standards.
8. Watson, C., "Modeling of Pressure Transients in Fuel Injection Lines," M.S. Thesis, School of Mechanical Engineering, Georgia Institute of Technology, Dec, 1999.
9. Yang, W. C. and Tobler, W.E. Dissipative modal approximation of fluid transmission lines using linear friction model. *Journal of Dynamic Systems, Measurement and Control,* 113, March 1991.